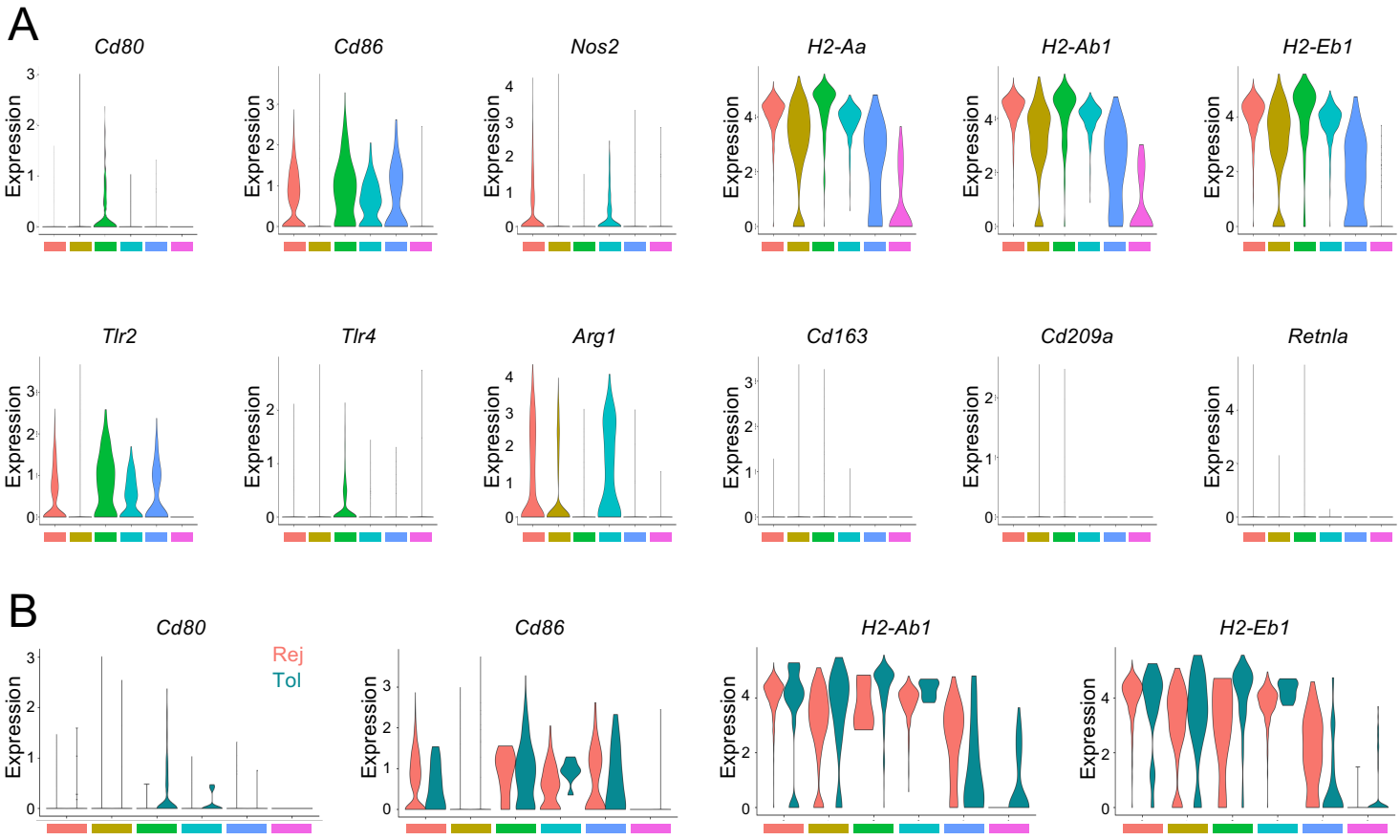


**Supplemental Figure 1. Expression of canonical "M1" or "M2" marker genes in macrophages during acute rejection or transplantation tolerance. A** Violin plots of M1 or M2 marker genes in macrophage and monocyte clusters in combined conditions identified in Figure 1C. **B** Violin plots of M1 or M2 markers genes in macrophage and monocyte clusters during acute rejection (Rej) or transplantation tolerance (Tol).

Cluster identification: *Pkm* MΦ, *Vegfa* MΦ, *Mrc1* MΦ, *Stat4* MΦ, *Nr4a1* mo, *Ly6c1* mo.

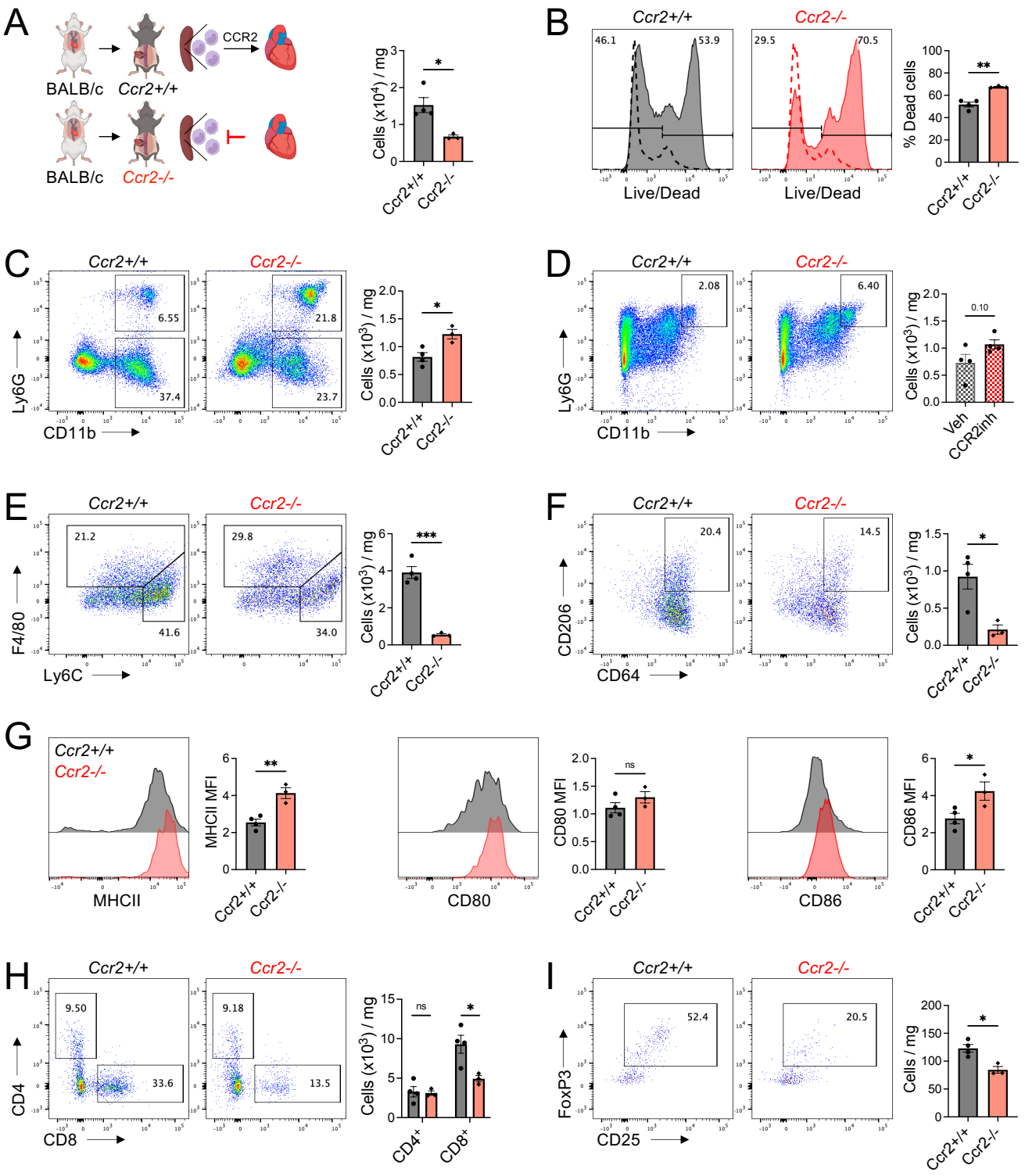


**Supplemental Figure 2. CCR2-dependent monocyte recruitment to cardiac allografts is required for transplantation tolerance.** Experimental design for heart transplantation in tolerized *Ccr2*+/+ or *Ccr2*-/- recipients with total abundance of **A** live or **B** dead cells in cardiac allografts 7 days after transplantation. Dashed lines in histograms represent splenocyte viability. Total abundance of **C and D** neutrophils, **E** Ly6C$^{hi}$ monocytes, and **F** CD206$^{+}$ macrophages in cardiac allografts 7 days after transplantation. **G** Expression of inflammatory markers on macrophages in cardiac allografts 7 days after transplantation. Total abundance of **H** CD4$^{+}$ T cells, CD8$^{+}$ T cells, and **I** FoxP3$^{+}$ T regulatory cells in cardiac allografts 7 days after transplantation. *n* = 3-4 mice/group pooled from 2 independent experiments. ns, not significant, **P*<0.05, ***P*<0.01, ***P*<0.001 by two-tailed, unpaired *t* test. All data represent mean ± SEM.

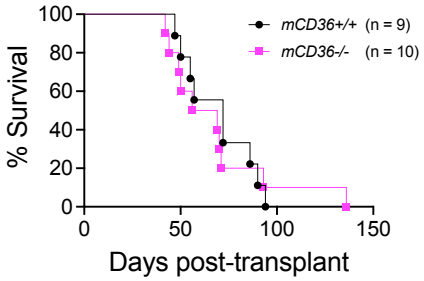


**Supplemental Figure 3. Myeloid cell expression of CD36 is dispensable for transplantation tolerance.** Cardiac allograft survival in tolerized *mCD36+/+ or mCD36-/-* recipients. *n* = 9-10 mice/group pooled from 3 independent experiments. Not significant by Log-rank (Mantel-Cox) test.

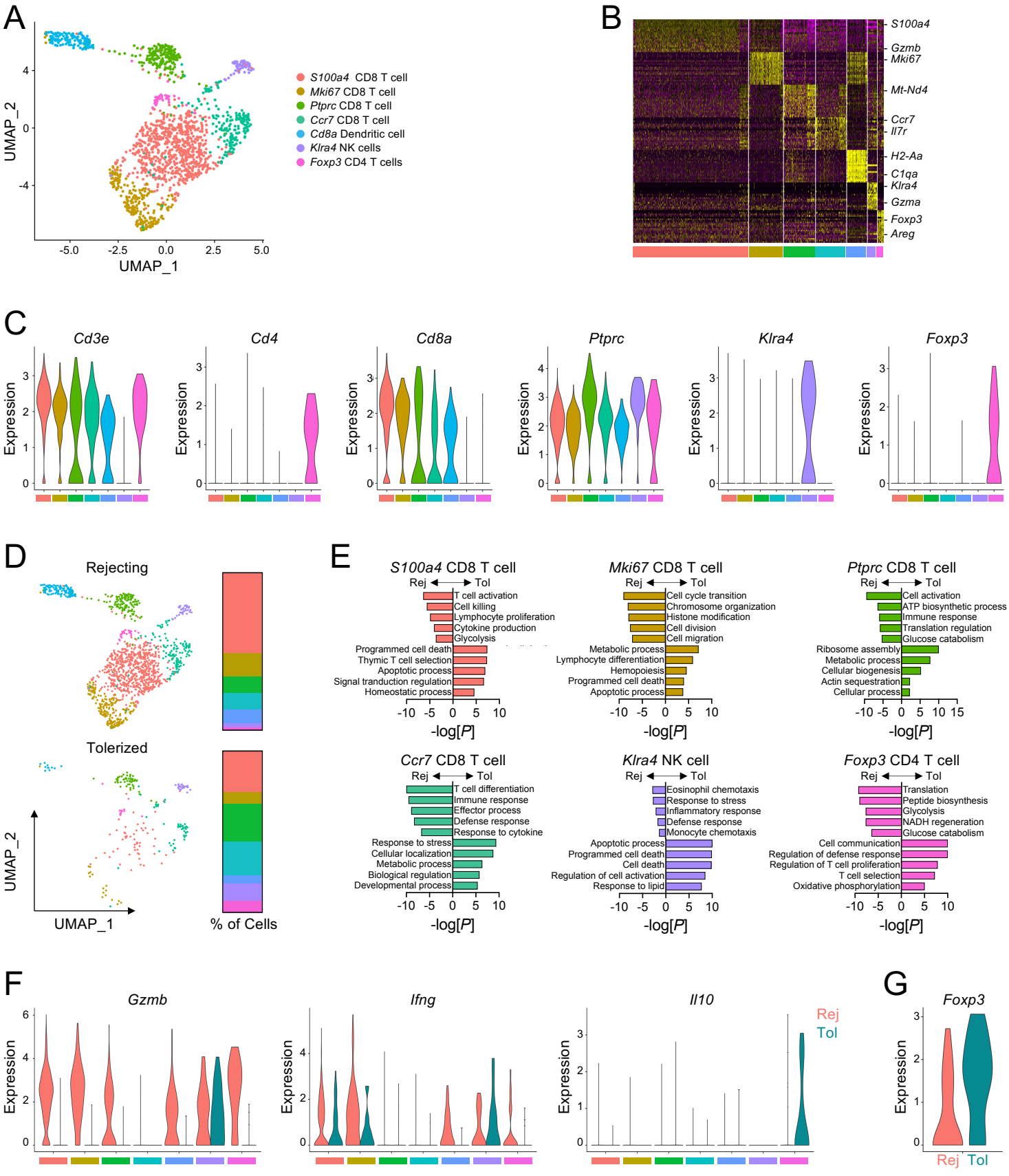


**Supplemental Figure 4. Single cell RNA sequencing of cardiac allografts during acute rejection or tolerance reveals unique populations of lymphocytes. A** Identification of 7 unique clusters by uniform manifold approximation and projection (UMAP) in combined conditions. **B** Heatmap of the 20 most differentially expressed genes within lymphocyte clusters. **C** Violin plots of lymphocyte marker genes. **D** Proportion of lymphocyte clusters present during acute rejection or tolerance. **E** Pathway enrichment of differentially expressed genes in lymphocyte clusters. Enrichment is expressed as the –log[*P*] and is adjusted for multiple comparisons. **F** Violin plots of genes expressed in lymphocyte clusters during acute rejection or tolerance. **G** Violin plot of *Foxp3* expression in *Foxp3* CD4 T cell cluster.

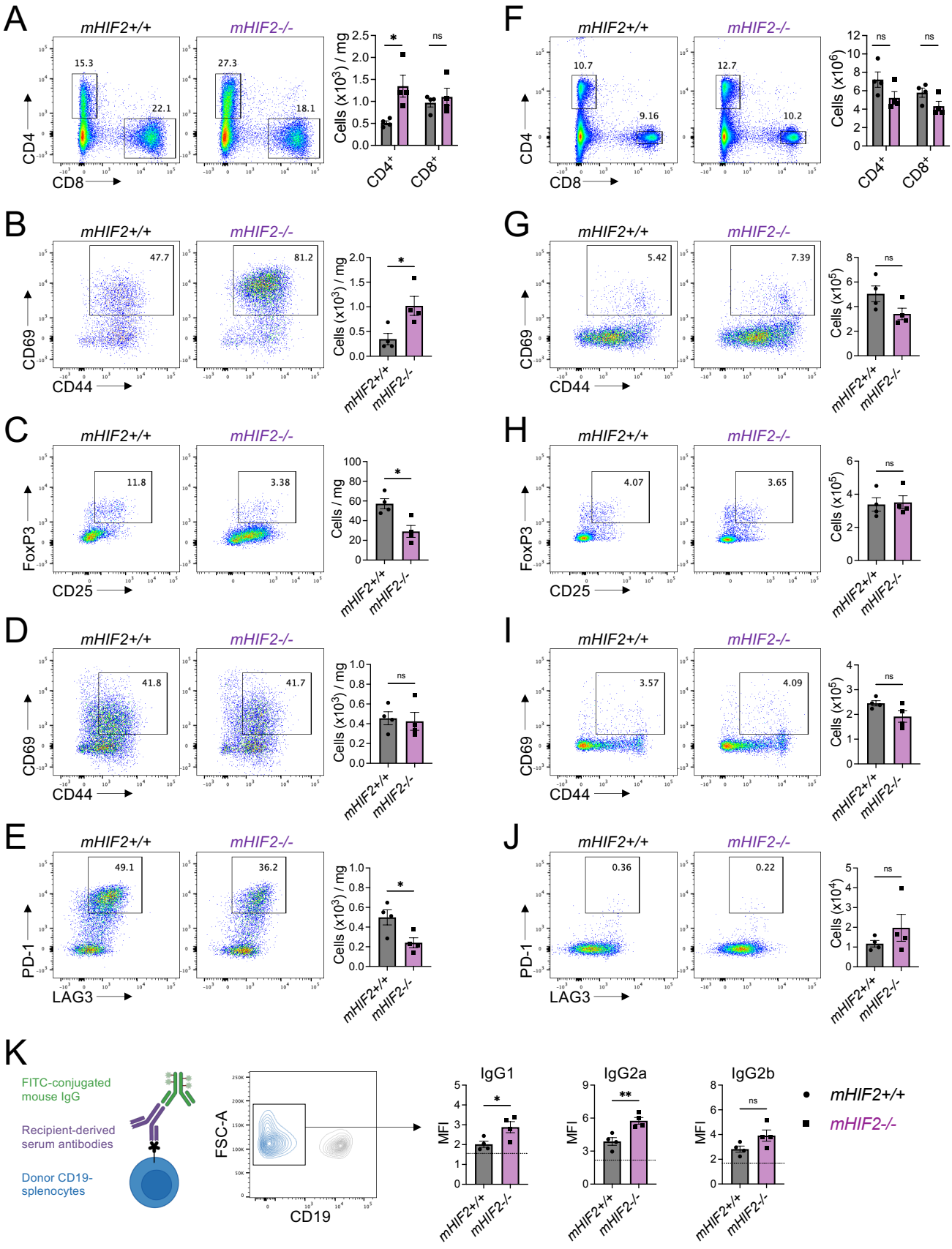


**Supplemental Figure 5. Myeloid HIF-2α is required to suppress effector T cell responses during cardiac allograft transplantation tolerance (cont. next page).**

**(Cont.) Supplemental Figure 5. Myeloid HIF-2α is required to suppress effector T cell responses during cardiac allograft transplantation tolerance. A** Total abundance of $CD4^+$ or $CD8^+$ T cells in cardiac allografts from tolerized *mHIF2+/+* or *mHIF2-/-* recipients 7 days after transplantation. *n* = 4 mice/group pooled from 2 independent experiments. **P*<0.05 by two-tailed, unpaired *t* test. Total abundance of **B** effector $CD44^+CD69^+$ $CD4^+$ T cells, **C** $FoxP3^+$ T regulatory cells, **D** effector $CD44^+CD69^+$ $CD8^+$ T cells, and **E** exhausted $LAG3^+PD\text{-}1^+$ $CD8^+$ T cells in cardiac allografts from tolerized *mHIF2+/+* or *mHIF2-/-* recipients 7 days after transplantation. *n* = 4 mice/group pooled from 2 independent experiments. **P*<0.05 by two-tailed, unpaired *t* test. **F** Total abundance of $CD4^+$ or $CD8^+$ T cells in spleens from tolerized *mHIF2+/+* or *mHIF2-/-* recipients 7 days after heart transplantation. *n* = 4 mice/group pooled from 2 independent experiments. ns, not significant by two-tailed, unpaired *t* test. Total abundance of **G** effector $CD44^+CD69^+$ $CD4^+$ T cells, **H** $FoxP3^+$ T regulatory cells, **I** effector $CD44^+CD69^+$ $CD8^+$ T cells, and **J** exhausted $LAG3^+PD\text{-}1^+$ $CD8^+$ T cells in spleens from tolerized *mHIF2+/+* or *mHIF2-/-* recipients 7 days after heart transplantation. *n* = 4 mice/group pooled from 2 independent experiments. ns, not significant by two-tailed, unpaired *t* test. **K** Donor specific antibodies in serum of tolerized *mHIF2+/+* or *mHIF2-/-* recipients 7 days after heart transplantation. Mean fluorescent intensity (MFI) for recipient-derived serum IgG1, IgG2a, or IgG2b antibodies was assessed on $CD19^-$ donor splenocytes. Dashed line represents no serum staining control. *n* = 4 mice/group pooled from 2 independent experiments. **P*<0.05, ***P*<0.01 by two-tailed, unpaired *t* test.

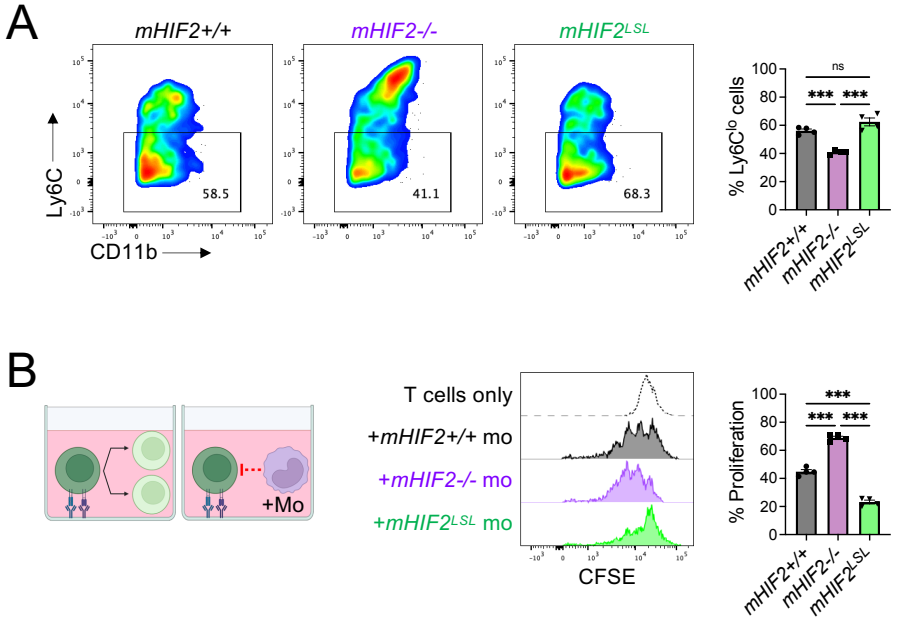


**Supplemental Figure 6. HIF-2α is required for monocyte-mediated suppression of T cell proliferation. A** Splenic Ly6C$^{hi}$ monocytes were enriched from mice treated with costimulatory blockade and donor spleen cells. Monocytes were cultured with M-CSF for 72 h and Ly6C expression was assessed by flow cytometry. Data are representative of two independent experiments. $n$ = 4 wells/group. ***$P$<0.001 by one-way ANOVA followed by Tukey's test. **B** Splenic monocytes (mo) were co-cultured with CFSE-labeled CD4$^+$ T cells at a ratio of 1:1 and proliferation was measured 3 days after anti-CD3/CD28 stimulation. Data are representative of two independent experiments. $n$ = 4 wells/group. ***$P$<0.001 by one-way ANOVA followed by Tukey's test. All data represent mean ± SEM.

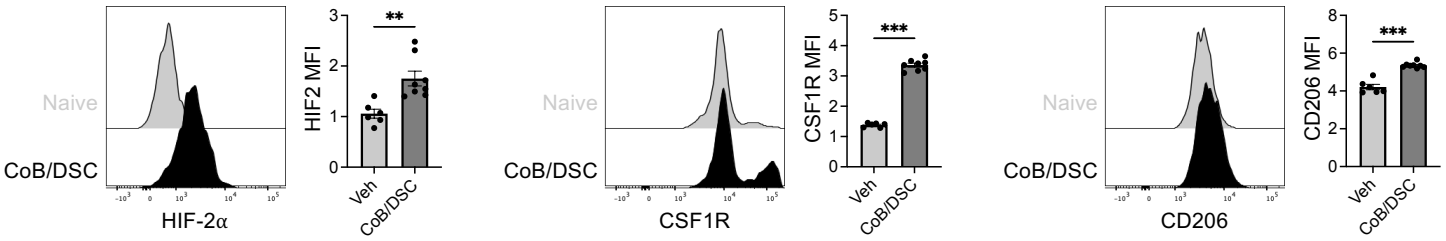


**Supplemental Figure 7. Co-culture of bone marrow-derived macrophages (BMDM) with costimulatory blockade (CoB) and donor splenocytes (DSC) increases HIF-2α levels.** Expression of HIF-2α, CSF1R, and CD206 in BMDMs co-cultured with CoB/DSC or vehicle. Data are representative of two independent experiments. *n* = 6-8 wells/group. ***P*<0.01, ****P*<0.001 by two-tailed, unpaired *t* test. Data represent mean ± SEM.

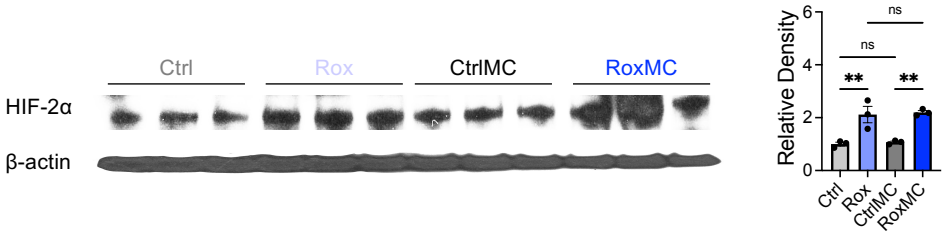


**Supplemental Figure 8. Roxadustat stabilizes HIF-2α in bone marrow-derived macrophages (BMDM).** Expression of HIF-2α in BMDMs treated with roxadustat (Rox) alone, roxadustat-loaded polyethylene glycol micelles (MC), or vehicle controls (Ctrl). Data are representative of two independent experiments. $n$ = 3 wells/group. $^{**}P<0.01$ by one-way ANOVA followed by Tukey's test. Data represent mean ± SEM.

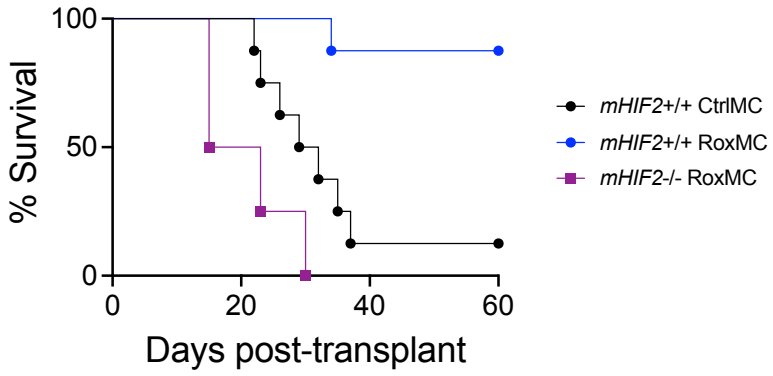


**Supplemental Figure 9. Myeloid HIF-2α is required for prolonged allograft survival after treatment with roxadustat-loaded micelles (RoxMC).** Cardiac allograft survival in *mHIF2*+/+ or *mHIF2-/-* recipients treated with CoB and RoxMC or control micelles (CtrlMC). *n* = 4-8 mice/group pooled from 3 independent experiments. Data for *mHIF2*+/+ CtrlMC and *mHIF2*+/+ RoxMC are the same as presented in Figure 8G.

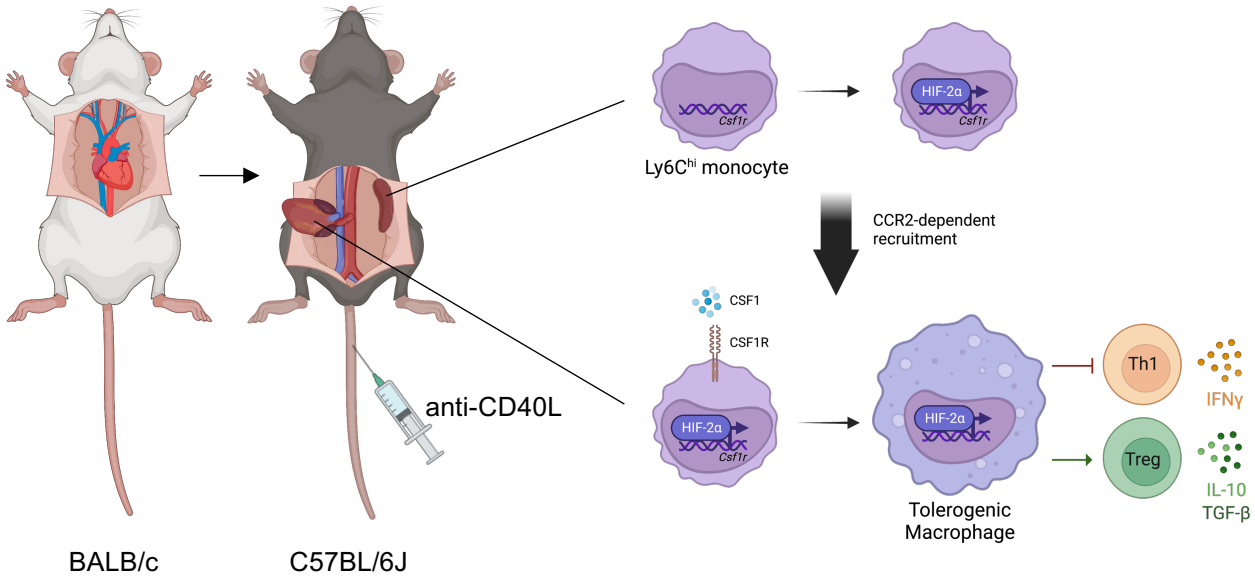


**Supplemental Figure 10. Hypoxia Inducible Factor (HIF)-2α promotes tolerogenic macrophage development during cardiac transplantation through transcriptional regulation of colony stimulating factor 1 receptor (CSF1R).** During heart transplantation with costimulatory blockade (anti-CD40L), HIF-2α is activated in splenic Ly6C$^{hi}$ monocytes leading to increased expression of *Csf1r*. These monocytes are then mobilized to the allograft through CCR2-dependent recruitment followed by CSF1-CSF1R signaling, which induces differentiation into tolerogenic macrophages capable of suppressing alloreactive Th1 responses and promoting allograft protective FoxP3$^{+}$ T regulatory (Treg) cells. Interferon-γ (IFNγ), Interleukin-10 (IL-10), Transforming Growth Factor-β (TGF-β)

## Methods

*Mice*

C57BL/6J mice (stock no. 000664) were purchased from Jackson Laboratory and bred in our animal facility before use as wild-type controls. Age- and sex-matched BALB/cJ mice (stock no: 000651) were used for donor hearts and purchased from Jackson Laboratory. *Ccr2* knockout mice (B6.129S4-Ccr2$^{tm1Ifc}$/J, stock no: 004999), *LysM-Cre* (B6.129P2-Lyz2$^{tm1(cre)Ifo}$/J, stock no. 004781), *HIF2*$^{flox/flox}$ (*Epas1*$^{tm1Mcs}$/J, stock no. 008407), and *CD36*$^{flox/flox}$ (Cd36$^{tm1.1Ijg}$/J, stock no: 032276) mice were purchased from Jackson Laboratory and backcrossed to wild-type C57BL/6J mice for 6–12 generations. To generate mice with myeloid lineage-specific knockout of CD36 (*mCD36-/-*) or HIF2 (*mHIF2-/-*), *LysM-Cre* mice were bred with *CD36*$^{flox/flox}$ or *HIF2*$^{flox/flox}$ mice, respectively. In experiments with *LysM-Cre* mice, mice that possessed the floxed gene but were *Cre* negative were used as controls. Mice with myeloid-specific overexpression of HIF-2$\alpha$ were generously provided by Dr. Yatrik Shah (University of Michigan, Ann Arbor, MI; (1). Mice were housed in temperature- and humidity-controlled, pathogen-free environments and kept on a 14:10 day/night cycle with access to standard mouse chow and water ad libitum. Two- to four-month-old male and female mice were used for experiments. Animal studies were conducted in accordance with guidelines using a protocol approved by the Institutional Animal Care and Use Committee at Northwestern University.

*Heterotopic Heart Transplantation*

Mice of B6 background were subjected to full MHC-mismatch abdominal heart transplantation as previously described (2, 3) in collaboration with Northwestern's Microsurgery and Preclinical Research Core. Briefly, hearts of age and sex-matched BALB/cJ donor mice were excised. Donor ascending aorta and pulmonary arteries were sutured to recipient abdominal aorta and inferior vena cava respectively. Complete anastomosis was confirmed through visualization of perfused donor cardiac tissue. Graft function was monitored three times per week by abdominal palpation. Rejection was defined as three consecutive measurements of a weak beat or complete cessation of a palpable beat.

*Transplantation Tolerance Induction*

For tolerance induction, mice received intravenous infusions of anti-CD40L antibody (500 µg per mouse) and donor BALB/c splenocytes (2 x $10^7$ cells) on day 0 prior to transplantation, followed by intraperitoneal injections of anti-CD40L (500µg per mouse) on days 7 and 14 post-transplantation as previously described (4, 5). Vehicle control mice received infusions of IgG control antibody of equivalent volume and frequency. For CCR2 inhibition, mice received intraperitoneal injections every other day of the selective CCR2 chemokine receptor antagonist, RS 504393 (2 mg/kg) or vehicle control. For experiments assessing the effect of roxadustat on allograft survival, mice received intraperitoneal injections of anti-CD40L antibody (250 µg per mouse) on days -7 and 0 for allograft rejection between days 20 to 40 post-transplantation (6).

*Tissue harvest*

Mice were euthanized by $CO_2$ asphyxiation, and allografts were extensively perfused by flushing the autologous left ventricle with a volume of 20 ml ice-cold PBS to remove peripheral cells. Allografts were excised from the abdominal aorta, weight, and transferred to a 1.5 ml microfuge tube. Allografts were then minced in Hanks Balanced Salt Solution containing Collagenase II (600U/mL; Sigma) and DNAse (60U/mL; Sigma) and digested at 37°C for 30 minutes. After digestion, the sample was processed through a 40$\mu$m filter to generate a single cell suspension. Whole spleens were harvested and subsequently triturated through a 40$\mu$m filter to prepare a single cell suspension. Samples were then subjected to RBC lysis, filtered again, and the number of viable cells was determined by counting cells on a hemocytometer with trypan blue exclusion.

*Immune Cell Enrichment*

For single cell RNA sequencing experiment, allograft cells were resuspended at $1x10^8$ cells/mL in EasySep buffer (StemCell). Samples were separated into two distinct selection procedures to enrich for either $CD45^+$ cells or pan-DCs according to manufacturer instructions (StemCell). Enriched cells were counted and re-pooled at a 1:1 ratio for single cell library preparation. For isolation of monocytes or $CD4^+$ T cells from spleens, splenocytes were resuspended at $1x10^8$ cells/mL in EasySep buffer (StemCell) and subjected to $Ly6C^{hi}$ monocyte or $CD4^+$ T cell immunomagnetic negative selection according to manufacturer instructions (StemCell).

*Single Cell Library Preparation and Sequencing*

For the single cell RNA sequencing experiment, 8-week-old, male C57BL/6J mice were subjected to heterotopic heart transplantation with tolerance induction protocol or vehicle control infusions (n = 4 mice/group). Allograft harvest was optimized such that time from mouse euthanasia to single cell library preparation was minimized and cells were maintained on ice throughout processing except for tissue digestion. Allografts were harvested according to predetermined endpoints (day 8 for acute rejecting allografts, day 40 for tolerized allografts) and biological replicates were pooled together by condition. Each condition was independently enriched for $CD45^+$ or $CD11c^+$ cells and enriched cells were re-pooled at a ratio of 1:1 for processing in the 10x Genomics Chromium System. Single cell mRNA sequencing libraries were prepared utilizing the 10X Genomics Chromium Next GEM Single Cell 3' Library and Gel Bead Kit (v3.1) pipeline following manufacturer protocols. A targeted number of 9,000 cells from the enriched cell suspension were loaded per experimental condition. RNA quality was confirmed utilizing Northwestern's NUSeq Core Agilent Bioanalyzer High Sensitivity Chip and Kapa Library Quantification Kits for Illumina platform (KAPA Biosystems). Libraries were sequenced on the HiSeq platform (Illumina) to a read depth of ~25,000 reads per cell by Novogene.

*Single Cell RNA Sequencing Analysis and Visualization*

Raw fastq files were analyzed using Cell Ranger version 4.2.2 (10X Genomics)(7). Barcode-gene matrices from Cell Ranger pipeline were analyzed using Seurat R package (v 4.3.0) (8). Low quality cells were removed if they expressed less than 500 unique molecular identifiers, less than 250 genes, or had a ratio of mitochondrial reads greater than 0.2. After quality control, a total of 4,027 or 1,167 individual cells from acute rejection or transplantation tolerance, respectively, were available for downstream bioinformatic analysis. Cell cycle heterogeneity was evaluated by calculation of cell cycle phase scores based on known markers and was regressed during data pre-processing (9). Normalization and variance stabilization was performed utilizing sctransform (v 0.3.5) (10). Single cell data sets from both conditions were then integrated utilizing cross-data set pairs of biological state "anchors" to minimize batch effects and allow for comparative scRNA-seq analysis between conditions (11). Principal component analysis (PCA) was performed to reduce dimensionality and subsequent applications employed a dimension of 40 principal components when necessary. Uniform manifold approximation and projection (UMAP) was utilized to visualize and unbiasedly cluster cells. Identification of clusters was initially performed using the unbiased SingleR algorithm which compares experimental data to reference transcriptomic data sets of pure cell populations (12). SingleR identifications were confirmed through assessment of canonical immune cell markers that were conserved across conditions. Differential expression tests were performed utilizing R package MAST (v 1.24.1) (13).

*Pathway Enrichment Analysis & Trajectory Inference*

Differentially expressed genes with adjusted p-values less than 0.05 were input into gProfiler to identify enriched molecular pathways within specific experimental processes. Gene sets from Gene Ontology Biological Process were utilized(14). Pseudotime trajectories of cell developmental identities within monocyte and macrophage identified clusters were assessed utilizing Monocle3 (v 1.3.1)(15). Gene expression and cellular trajectories across pseudotime were further analyzed and visualized utilizing Slingshot (v 2.6.0)(16).

*Immunofluorescence*

Fixed-frozen 10 μm sections were prepared from cardiac allografts. Sections were thawed and washed in PBS. Antigen retrieval was performed by heating sections for 20 minutes at 125°C and 22 psi in citrate buffer, pH 6.0 using a Decloaking Chamber (Biocare Medical). Sections were blocked for 1 hour at room temperature in TBS with 5% normal goat serum and 0.3% Triton X-100. Primary antibodies for CD11b (1:100; Biolegend) and CSF1R (1:100; Biolegend) were diluted in blocking buffer and incubated overnight at 4°C in a humidified staining tray. Sections were washed extensively in TBS-Tween and incubated with Alexa Fluor 488 goat anti-rat (1:100) and Alexa Fluor 594 goat anti-mouse (1:100) secondary antibodies diluted in TBS with 1% BSA and 0.3% Triton X-100 for 1 hour at room temperature in a dark humidified staining tray. Sections were washed extensively in TBS-Tween and mounted with a coverslip using Vectashield antifade mounting medium with DAPI. Alternatively, after antigen retrieval and blocking, sections were stained with FITC-conjugated anti-α-SMA antibody (1:100; F3777, Sigma) for 1 hour at room temperature in a dark humidified staining tray, washed, and mounted using Vectashield antifade mounting medium with DAPI. Sections were imaged at 20x magnification using a Slideview VS200 slide scanner (Olympus). Quantifications of cells and mean fluorescent intensity were performed using QuPath software.

*Flow Cytometry*

Single cell suspensions were resuspended in FACS buffer (PBS, 2% FBS, 2 mM EDTA). After washing in FACS buffer, dead cells were labeled by incubating samples with Zombie Aqua Fixable Dye (1:1,000; Biolegend) in PBS for 15 minutes at room temperature in the dark. Cells were washed in FACS buffer and blocked using TruStain FcX antibody (1:100; Biolegend) in FACS buffer for 15 minutes on ice. Cells were incubated with primary antibodies (1:200 dilution) in FACS buffer for 20 minutes on ice in the dark. For intracellular staining, cells were first stained with surface antibodies, fixed and permeabilized using True-Nuclear Transcription Factor buffer set (Biolegend), and then incubated with antibodies for HIF-2α (1:50; Novus Bio) or FoxP3 (1:50; eBioscience) in True-Nuclear permeabilization buffer for 30 minutes at room temperature in the dark. Flow cytometric analyses were performed on a LSRFortessa X-20 Cell Analyzer (BD Biosciences). BD Compbeads (BD Biosciences) were used to optimize fluorescence compensation settings to enable multicolor flow cytometric analyses. Fluorescent minus one and gene-deleted mice or cells were used as staining controls. All cells were pregated on live (live-dead exclusion), single cells. Data were analyzed on FlowJo software (Tree Star).

*Donor specific antibodies*

Spleens from BALB/c mice were harvested and processed into single cell suspensions using a 40 μm filter. Following RBC lysis, $1x10^6$ splenocytes were incubated with 3 μL of serum from recipient mice for 1 hour at 4°C. Cells were washed incubated with PE-conjugated anti-CD19 and FITC-conjugated antibody to either anti-mouse IgG1, IgG2a, or IgG2b for 30 minutes 4°C. Using flow cytometry, donor specific antibodies were quantified as the mean fluorescent intensity of FITC on CD19-negative cells.

*CoB/DSC treatment*

To measure acute responses to CoB/DSC treatment, mice received a single intravenous injection of anti-CD40L antibody (500 µg per mouse) and donor BALB/c splenocytes (5 x $10^7$ cells). Spleens were harvested 72 hours later and processed into single cells suspensions using a 40 µm filter. Splenocytes were then processed for either flow cytometry or Ly6C$^{hi}$ monocytes were enriched using immunomagnetic negative selection. For in vitro experiments, RBC lysed BALB/c splenocytes were co-cultured with bone marrow-derived macrophages (2.5x$10^5$ cells/well) at a ratio of 2 splenocytes : 1 macrophage. Anti-CD40L antibody was added at a concentration of 50 µg/mL as previously described (17). Cells were cultured for 3 hours prior to harvest for surface and intracellular staining for flow cytometry.

*T cell suppression assay*

After processing spleens from C57BL/6J mice into single cell suspensions, CD4$^+$ T cells were enriched by immunomagnetic negative selection. The enriched CD4$^+$ T cells were labeled with 5 µM CFSE, washed, and transferred to 96-well tissue culture plates coated with anti-CD3 (1 µg/ml) and anti-CD28 (2 µg/ml) antibodies for stimulation. CD4$^+$ T cells were co-cultured with splenic Ly6C$^{hi}$ monocytes enriched from CoB/DSC treated mice at a ratio of 1:1 in RPMI media supplemented with 10% fetal bovine serum, L-Glutamine, sodium pyruvate, and penicillin-streptomycin. Following 4 days of co-culture, flow cytometry was used to assess CSFE dilution in CD4$^+$ T cells and Ly6C expression on monocytes.

*Chromatin Immunoprecipitation*

After processing spleens and isolating Ly6C$^{hi}$ monocytes from CoB/DSC treated mice or controls, 5x$10^5$ cells were processed for chromatin immunoprecipitation using a High-Sensitivity ChIP Kit (Abcam). Following fixation and lysis, chromatin was sheared by sonication with 4 pulses of 15 seconds each at 25% power with a rest of 30 seconds on ice between each pulse. Sheared chromatin (2 µg/well) was incubated with anti-mouse HIF-2α antibody (0.8 µg/well ; Novus) or non-immune IgG control antibody (0.8 µg/well; Abcam) at 4°C overnight. Crosslinks were reversed and DNA was released and purified before using 2 µL of eluted DNA for real time PCR analysis. HREs were identified using the consensus sequence 5'-ACGTG-3', and the following primers were used for real time PCR analysis:

HRE1-F (5'-GTGTTGCAAAGAGGGCATCG-3')
HRE1-R (5'- CAGAGCACACCGTGAGTCAA-3')
HRE2-F (5'-ATTTCCAAATTCTGTAGTTCCCTTT-3')
HRE2-R (5'-GCTAGTTCTGTGAGGACGGG-3')
HRE3-F (5'-TAGTGATCAGCGTGCTTCCC-3')
HRE3-R (5'-GGGCTGACGAATTCCACGTA-3')

Fold enrichment was calculated by using a ratio of amplification efficiency of the ChiP sample over that of non-immune IgG control.

*Roxadustat treatment*

Roxadustat (Tocris) was encapsulated in spherical micelles, assembled from poly(ethylene glycol)-poly(propylene sulfide) (PEG-PPS) block copolymers. The synthesis of $PEG_{45}$-$PPS_{36}$ block copolymer was performed as described previously (18, 19). In a typical roxadustat loading experiment, 1.2 mL of water was added dropwise (10 µL/step) into 1 mL of N,N-dimethylformamide (DMF) solution of PEG-PPS (40 mg) and roxadustat (2 mg) under stirring. The mixture was dialyzed in water to remove DMF, followed by filtration using a 200 nm syringe filter. Based on fluorescence quantification ($\lambda_{ex}$ = 364 nm, $\lambda_{em}$ = 409 nm), encapsulation efficiency was at least 70%. For HIF-2α activation in vitro, bone marrow-derived macrophages

($2.5x10^5$ cells/well) were treated with 20 μM roxadustat alone or within PEG-PPS micelles for 6 hours. DMSO and unloaded PEG-PPS micelles were used as controls. HIF-2α levels were determined by immunoblot and relative band density was normalized to β-actin. For splenic monocyte HIF-2$\alpha$ activation in vivo, mice were treated with roxadustat (50 mg/kg) or vehicle control (DMSO) in PBS by intraperitoneal injection every other day for 1 week. Alternatively, mice received 1.8 mg/kg roxadustat encapsulated in PEG-PPS micelles or unloaded PEG-PPS micelles as control by intraperitoneal injection every other day for 1 week. After euthanasia, plasma was collected into EDTA coated tubes through cardiac puncture. Spleens were harvested and processed into single cell suspensions for flow cytometric analyses. For experiments assessing the effect of roxadustat on allograft survival, mice received 1.8 mg/kg of roxadustat encapsulated in PEG-PPS micelles or unloaded PEG-PPS micelles on days -7 and 0 of transplant.

*Statistical Analyses*

Statistical analyses were performed with GraphPad Prism 10 software (GraphPad Software). Comparisons between two groups were performed using a two-tailed, unpaired *t* test with a 95% confidence interval. For comparisons of more than two variables, a one-way or two-way ANOVA was used with a 95% confidence interval; when necessary, a Tukey test was used to correct for multiple comparisons. The statistical difference in allograft survival was determined by a log-rank (Mantel–Cox) test. For in vivo experiments, experimental sample size is indicated in figure and figure legends and represent pooled data from two or more independent experiments. For in vitro experiments, experimental sample size is indicated in figure and figure legends and are representative data from two or more independent experiments. All data are presented as mean ± SEM. Criteria for significant differences (*$P$<0.05, **$P$<0.01, ***$P$<0.001) are in the figure legends. Analyses labeled “ns” are not statistically significant.

These studies used sequencing services provided by NUSeq Core and microsurgical services provided by Microsurgery and Preclinical Research Core at Northwestern University. Figure schematics were created with Biorender.com.

## References

1. L. Xie *et al.*, Hypoxia-inducible factor/MAZ-dependent induction of caveolin-1 regulates colon permeability through suppression of occludin, leading to hypoxia-induced inflammation. **34**, 3013-3023 (2014).
2. T. Hasegawa, S. H. Visovatti, M. C. Hyman, T. Hayasaki, D. J. Pinsky, Heterotopic vascularized murine cardiac transplantation to study graft arteriopathy. *Nat Protoc* **2**, 471-480 (2007).
3. K. Glinton *et al.*, Bone Marrow-Derived AXL Tyrosine Kinase Promotes Mitogenic Crosstalk and Cardiac Allograft Vasculopathy. *bioRxiv* 10.1101/2021.02.04.429773, 2021.2002.2004.429773 (2021).
4. M. L. Miller *et al.*, Spontaneous restoration of transplantation tolerance after acute rejection. *Nat Commun* **6**, 7566 (2015).
5. S. H. Khiew *et al.*, Transplantation tolerance modifies donor-specific B cell fate to suppress de novo alloreactive B cells. *J Clin Invest* **130**, 3453-3466 (2020).
6. P. Björck, P. T. H. Coates, Z. Wang, F. J. Duncan, A. W. Thomson, Promotion of Long-Term Heart Allograft Survival by Combination of Mobilized Donor Plasmacytoid Dendritic Cells and Anti-CD154 Monoclonal Antibody. *The Journal of Heart and Lung Transplantation* **24**, 1118-1120 (2005).
7. G. X. Zheng *et al.*, Massively parallel digital transcriptional profiling of single cells. *Nat Commun* **8**, 14049 (2017).

8. Y. Hao *et al.*, Integrated analysis of multimodal single-cell data. *Cell* **184**, 3573-3587.e3529 (2021).
9. S. Nestorowa *et al.*, A single-cell resolution map of mouse hematopoietic stem and progenitor cell differentiation. *Blood* **128**, e20-31 (2016).
10. C. Hafemeister, R. Satija, Normalization and variance stabilization of single-cell RNA-seq data using regularized negative binomial regression. *Genome Biol* **20**, 296 (2019).
11. T. Stuart *et al.*, Comprehensive Integration of Single-Cell Data. *Cell* **177**, 1888-1902.e1821 (2019).
12. D. Aran *et al.*, Reference-based analysis of lung single-cell sequencing reveals a transitional profibrotic macrophage. *Nat Immunol* **20**, 163-172 (2019).
13. M. A. Finak G, Yajima M, Deng J, Gersuk V, Shalek AK, Slichter CK, Miller HW, McElrath MJ, Prlic M, Linsley PS, Gottardo R., MAST: a flexible statistical framework for assessing transcriptional changes and characterizing heterogeneity in single-cell RNA sequencing data. *Genome Biol* 10.1186/s13059-015-0844-5 (2015 Dec 10).
14. U. Raudvere *et al.*, g:Profiler: a web server for functional enrichment analysis and conversions of gene lists (2019 update). *Nucleic Acids Res* **47**, W191-w198 (2019).
15. C. Trapnell *et al.*, The dynamics and regulators of cell fate decisions are revealed by pseudotemporal ordering of single cells. *Nat Biotechnol* **32**, 381-386 (2014).
16. K. Street *et al.*, Slingshot: cell lineage and pseudotime inference for single-cell transcriptomics. *BMC Genomics* **19**, 477 (2018).
17. P. A. Taylor, A. Panoskaltsis-Mortari, R. J. Noelle, B. R. Blazar, Analysis of the Requirements for the Induction of CD4+ T Cell Alloantigen Hyporesponsiveness by Ex Vivo Anti-CD40 Ligand Antibody1. *The Journal of Immunology* **164**, 612-622 (2000).
18. S. Allen, O. Osorio, Y.-G. Liu, E. Scott, Facile assembly and loading of theranostic polymersomes via multi-impingement flash nanoprecipitation. *Journal of Controlled Release* **262**, 91-103 (2017).
19. S. Au - Allen, M. Au - Vincent, E. Au - Scott, Rapid, Scalable Assembly and Loading of Bioactive Proteins and Immunostimulants into Diverse Synthetic Nanocarriers Via Flash Nanoprecipitation. *JoVE* doi:10.3791/57793, e57793 (2018).